J Mater Sci (2007) 42:5613–5619
DOI 10.1007/s10853-006-1116-2

Mechanical vs. electrical failure mechanisms in high voltage, high energy density multilayer ceramic capacitors

Amanda Lynn Young · Gregory E. Hilmas · Shi C. Zhang · Robert W. Schwartz

Received: 4 April 2006 / Accepted: 10 October 2006 / Published online: 6 April 2007

Abstract Causes of breakdown, both mechanical and electrical, in high voltage, high energy density, $BaTiO_3$ capacitors were studied. The flexural strength of the capacitors was 96 MPa. Failure was due to surface defects or pores close to the surfaces of the samples. The dielectric breakdown strength of the samples was 181 kV/cm. The causes of breakdown were either electrode end effects or pores between the dielectric and electrode layers. Weibull statistics were used to determine if there was a correlation between mechanical failure and dielectric breakdown. A strong correlation between the two types of failure was not found in the study, in contrast to earlier studies of single dielectric layer capacitor materials.

Introduction

New applications for multilayer ceramic capacitors are driving the need for materials that have a high dielectric energy density and reliability, specifically pulsed power applications, including high power microwave and electromagnetic (EM) gun technologies [1]. The equation for the dielectric energy density in a material can be given as:

$$J = \int_0^{E_{max}} \varepsilon_0 \varepsilon(E) E dE \quad (1)$$

where J is the energy density (J/m^3), E is the applied electric field (V/m), ε is the relative permittivity and ε_0 is the permittivity of free space (F/m). Equation (1) accounts for the field dependence of the dielectric constant that is observed for ferroelectric materials. Assuming that the material does not demonstrate field-dependence of the dielectric constant, the following equation may be derived:

$$J = 1/2\ \varepsilon_0 k'(V/t)^2 \quad (2)$$

where J is the volumetric energy density, ε_0 is the permittivity of free space, k' is the dielectric constant, V is the applied voltage, and t is the dielectric layer thickness. A capacitor must possess a high dielectric constant and layers that are as thin as possible in order to increase energy density.

To improve the performance of multilayer capacitors, along with obtaining a high permittivity, the mechanisms of breakdown in these laminate architectures, both mechanical and electrical, must be understood. After the breakdown mechanisms are understood, methods can then be implemented to minimize or eliminate breakdown and thus improve the performance of the capacitors through the $(V/t)^2$ term.

Dielectric breakdown strength

Dielectric breakdown is a well-known phenomenon that occurs in multilayer ceramic capacitors, and the causes of dielectric breakdown in ferroelectric ceramics have been widely studied [2]. Three breakdown mechanisms are commonly accepted for solids: intrinsic breakdown, thermal breakdown and ionization breakdown [3–5].

The dielectric strength depends on many factors, including material parameters such as porosity and grain

A. L. Young (✉) · G. E. Hilmas · S. C. Zhang · R. W. Schwartz
Department of Materials Science and Engineering, University of Missouri-Rolla, 222 McNutt Hall, Rolla, MO 65409, USA
e-mail: ayoung@umr.edu

G. E. Hilmas
e-mail: ghilmas@umr.edu

size, and external parameters, such as the frequency and ramp rate of the applied voltage. The effect of porosity on the dielectric strength of materials has also been widely reported in the literature. Beauchamp demonstrated a decrease in breakdown strength with increasing porosity, with the breakdown strength decreasing by a factor of approximately 3 with a 12% increase in porosity [6]. Gerson used a statistical approach to show trends in breakdown strength as the amount of porosity was altered [7]. In his proposed model, Gerson assumed that all of the voids were of equal size and uniformly distributed in the material. Again, the breakdown strength decreased abruptly, from a breakdown strength of 79 kV/cm for a fully dense material to approximately 20 kV/cm at 22% porosity. The trends in porosity showed that, if present in the material, pores were likely the main cause of failure of multilayer ceramic capacitors.

Besides porosity, many other factors contribute to dielectric breakdown in multilayer ceramic capacitors. Thermal runaway can be a cause of breakdown in ceramic materials [8]. Localized reduction of the ceramic dielectric occurs leading to an increase in conductivity. Heating causes a rapid rise in temperature and results in melting of the ceramic which can cause a conduction path to form between the electrodes and hence cause breakdown. The tapered geometry of electrode ends is known to result in a field enhancement effect that can lead to premature breakdown due to higher field intensity near these regions [9]. Basically, breakdown occurs at lower applied fields than expected as a result of field enhancement. Mechanical defects, such as cracks, can also lead to premature failure [10]. Ferroelectrics commonly fracture due to the application of high fields. Due to the design of multilayer capacitors, each layer is clamped at its edge which can lead to electric field-induced mechanical stresses leading to cracks and failure [11]. Another cause of cracks in ceramics can be due to edge effects of the electrodes [12]. The electrodes end inside the material which can cause a strain incompatibility due to the inactive material being next to the active material. This can create a stress field at the electrode edge which can lead to crack initiation at this site. Mechanical stresses can further lead to crack initiation and growth and finally failure in the device. Electrical shorts can be also be caused by cracks perpendicular to the interface of the capacitor between the dielectric and electrode layers. Overall, any field-enhancing defect present in the capacitor can lead to dielectric breakdown.

Besides internal defects, extrinsic conditions can also affect the breakdown strength of a material. The extrinsic factor that is believed to be the most common cause of a reduction in breakdown strength is moisture adsorption [13]. Thus, the electrical failure of a dielectric material can be due to a combination of competing factors, both intrinsic and extrinsic.

Mechanical strength

Ceramics have wide distributions in failure strength. The response of a solid to an applied stress is deformation (linear assuming low stresses applied under reversible conditions). However, if the applied stress exceeds the strength of the material, it will fail mechanically [14]. Mechanical failure occurs in multilayer ceramic capacitors, but it has been rarely investigated, and is certainly not as well studied as dielectric breakdown. Mechanical failure is common in high voltage, high energy density multilayer capacitors and occurs for several different reasons. As large capacitors are discharged, a ringing effect will take place within a ferroelectric material [15]. A large peak current occurs during this discharge event, which in turn leads to high mechanical stresses, especially in large capacitors [15]. A second type of failure mechanism in ceramic capacitors, specifically $BaTiO_3$, is due to large residual stresses from the phase transformation that occurs during cooling the material from the sintering temperature to room temperature [16]. When the material is above the Curie temperature, the material is cubic and therefore internal stresses and ferroelastic twinning are absent. As the material is cooled through the Curie transition, large residual stresses develop during the transformation from the cubic to the tetragonal phase, which weakens the material, leading to failure at measurably reduced strengths. Strength degradation can also occur due to the presence of microstructural defects such as pores and machining flaws. Mechanical properties, including the elastic modulus and flexural strength, of materials are known to decrease as the porosity level increases [14]. Surface defects, possibly due to machining and handling, can also be a major source of stress concentrations, resulting in failure at lower strengths.

Weibull statistics

A statistical distribution commonly used to represent the strength of brittle materials is that proposed by Weibull [17]. The use of Weibull plots to compare mechanical failure data with electrical breakdown data in $BaTiO_3$ ceramics has been pointed out by Kishimoto [18]. Weibull plots have also been successfully used to compare mechanical and electrical strength data for other materials such as hardened gypsum [19]. Weibull statistics can be used to plot the distributions for both the mechanical and electrical property data. Calculated Weibull moduli, determined from the distributions, provide a statistical

comparison of the distribution in the mechanical and electrical strength values. Similar electrical and mechanical failure distributions and Weibull moduli have been interpreted as an indication of similar failure origins in $BaTiO_3$ ceramics [18]. The study of Kishimoto suggested that Weibull plots may be used effectively to determine if there is a correlation between mechanical failure and dielectric breakdown in electrical ceramics.

The purpose of this paper is to measure the mechanical and electrical breakdown strength of $BaTiO_3$ in high voltage, high energy density multilayer ceramic capacitors. Weibull statistics, along with the identification of both the electrical and mechanical failure origins, will be used to determine if there is a correlation between mechanical and electrical failure in the capacitors. Unlike the prior study by Kishimoto, which reported the behavior of single dielectric layer capacitors, this work focuses on the behavior of multilayer ceramic capacitor devices.

Experimental procedure

Test bars for both mechanical flexure testing and electrical breakdown strength measurements were produced by tape casting dielectric sheets and screen printing the electrode geometry. The tape casting slurries were prepared using a standard 58 vol.% dielectric powder (Ferro X7R 422H, $BaTiO_3$ based material) and 42 vol.% binder (Ferro B73210). The powder and binder solution were ball milled using ZrO_2 milling media for 48 h. The slurry was then filtered using a 5 μm filter to remove any agglomerates in the slurry, de-aired at 15 mm Hg for 5 min, and slow rolled for 24 h to assure a homogeneous mixture. The tape was cast on silicone coated mylar at a thickness of 0.05 mm (20 mils) and dried for 1 h (~0.015 mm thickness (6 mils) after drying). The tape was then cut into 139.7 mm × 139.7 mm (5.5″ × 5.5″) squares for further processing.

The tape cast sheets for the bars were screen printed with 30Ag/70Pd ink (Ferro EL 44006) using an Aremco Accu-coat screen printing machine. A total of 28 sheets (12 electrode layers and 16 blank (not screen printed)) layers were aligned and stacked to produce test bars for mechanical flexure testing. The bars were fabricated so that they would function as working capacitors. All of the samples underwent the same lamination conditions: 85 °C and 2.8 MPa (400 psi) for 10 min. The final thickness after lamination was approximately 4.0 mm. After lamination, 10 mm × 4.0 mm × 60 mm bars were cut from the large stack. The bars underwent burnout in air at 5 °C/h to a maximum temperature of 500 °C to remove all of the remaining organic binder. After burnout, the samples were sintered by heating at 5 °C/min to 1,300 °C, held for 2 h, and furnace cooled at 10 °C/min to room temperature. The sintered bars for mechanical testing were polished from a 3 μm to 0.25 μm diamond finish and tested using a four-point bend method. The polished surface minimizes the likelihood of failures originating at surface defects typical of as-sintered surfaces. Removal of the surface or near-surface defects also allows some of the bulk of the $BaTiO_3$ dielectric to be tested so that all of the failures do not arise from extrinsic defects on the as-sintered surface. This allows for comparison with the breakdown data, since breakdown tests the bulk of the material, not the surface. Figure 1 shows the area of the bar that is being tested in flexure. Figure 2 shows the area of the bar that will be tested electrically. The final dimensions of the bars were approximately 45 mm × 8 mm × 3 mm.

A fully articulated four-point bend fixture was used for mechanical testing according to ASTM Standard C1161-02c. Mechanical testing was performed using a screw-driven Instron testing machine (Instron Model 4204, Norwood, MA) using a crosshead speed of 0.5 mm/min (strain rate of 0.0056/min and a stressing rate of 0.5625 GPa/min). The outer span of the four-point bend fixture was 40 mm and the inner span was 20 mm for all of the flexure strength tests. The flexure strengths were then calculated using a standard four-point bend equation. A total of 30 bars were tested mechanically in order to obtain statistical data.

The same bar geometry was used for both the electrical measurements and the mechanical measurements. The bars with internal electrodes were terminated with Ag ink, heated at 5 °C/min to 700 °C, and held for 10 min after coating to sinter the termination material. The bars for mechanical testing were also heated to 700 °C prior to testing to assure that the bars were processed identically

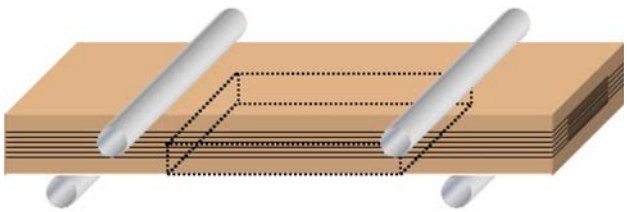

Fig. 1 Schematic of the volume of the bar being tested using a four-point bend method

Fig. 2 Schematic of the volume of the bar being tested electrically

and therefore could be directly compared. The capacitance was measured with a Hewlett Packard 4192A LF Impedance Analyzer at a frequency of 1 kHz and 1 volt. The breakdown measurements were made with a Hewlett Packard 4104B DC voltage source and a Trek Model 20120A Amplifier. The bars were immersed in Fluorinert fluid for breakdown testing to suppress surface breakdown. A total of 30 bars were tested electrically in order to obtain statistically significant data.

Results

Strength measurements

The electrode-containing bars were found to have an average flexural strength of 96 ± 13 MPa. The results of this experiment show that $BaTiO_3$ is a much weaker material than oxide ceramics such as Al_2O_3 or ZrO_2. The strength level is consistent with values previously determined for similar electrical ceramic materials such as $BaTiO_3$, PZT and ZnO. Al-Saffar et al. [20] studied the flexure strength of $BaTiO_3$ multilayer ceramic capacitors with varying thicknesses. The flexural strength of a 0.90 mm thick X7R bar was 136 MPa, whereas a 1.33 mm thick bar had a flexural strength of only 119 MPa. The capacitors in this study were 3 mm thick; therefore, the strength of the bars correlates well with the literature values for $BaTiO_3$.

Table 1 shows the results for the electrical property measurements of the bars produced in this study. The average dielectric constant was 3,933 and the average breakdown strength was 181 ± 11 kV/cm (459 volts/mil). The dielectric constant was well within the range expected, which is approximately 4,000, for X7R-based materials [21]. The breakdown strength was lower than values quoted by the manufacturer (276 kV/cm or 700 V/mil) for this X7R-based material. This variation is expected based on the large size of the bars being tested as compared to the quoted value from the manufacturer which was likely determined on thin (~25 μm) single layer samples. The breakdown strength could also vary due to the ramp rates and test conditions that were used for the current experiments.

It is well known that the probability of a larger flaw being present increases as the volume of material under uniform stress increases, leading to lower measured strengths for larger components [17]. However, it is also well known that once the volume of a material has increased to a particular level, there is a nearly 100% probability that a component will contain a flaw of the appropriate critical size, such that any further increase in volume (or thickness given the same length and width dimensions) will not significantly reduce the failure strength. Thus, there is a clear trend of decreasing strength, both mechanical and electrical, with increasing dielectric thickness, but at some thickness (volume), the strength values will become nearly constant.

Comparison between mechanical and electrical breakdown events (Weibull)

A comparison of the Weibull plots for the two sets of bars, as sintered bars for electrical breakdown and polished bars for flexure strength, is shown in Fig. 3. The Weibull plots have been normalized using the average strength reported above so that the results can be plotted on the same graph for ease of comparison. The Weibull modulus for the flexure tests is 10, whereas for the electrical breakdown measurements, a Weibull modulus of 18 is observed. The shape of the distributions is also dissimilar. Based on these results, there does not appear to be a strong correlation between electrical breakdown and mechanical failure in large sized high voltage, high energy density capacitors. We have to keep in mind that the latter conclusion is based solely on the comparison of electrical breakdown to ''flexure'' testing.

These results are in contrast to those of Kishimoto who suggested the existence of a strong correlation between mechanical and electrical breakdown in $BaTiO_3$ ceramics sintered at 1,350 °C (Fig. 4 of ref. [18]) based on the comparison of the Weibull distributions of the electrical and mechanical strength. Data from Kishimoto (repeated herein as Fig. 4) shows the statistical probability for both the mechanical and electrical failure to be nearly identical. The Weibull moduli for both the mechanical plot and the electrical plot are similar, with a value of approximately 5. In addition, Kishimoto suggested that the failure origins and population of failures in both mechanical failure and electrical breakdown are the same. He also suggested that the microstructure of the material plays a strong role in both mechanical and electrical failure. In order to under-

Table 1 Results of the electrical measurements

Sample	Dielectric constant	Dissipation factor (%)	Average breakdown strength (kV/cm)	Std. Dev.
As-sintered (30 sample average)	3,933	0.69	181	11

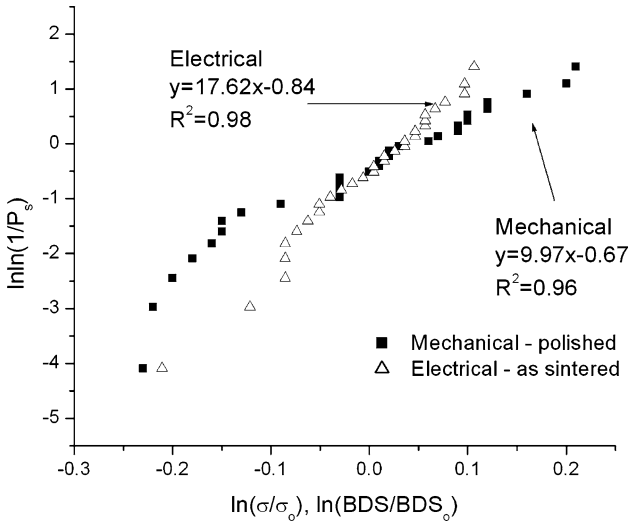

Fig. 3 Weibull plot containing both mechanical strength and electrical breakdown data

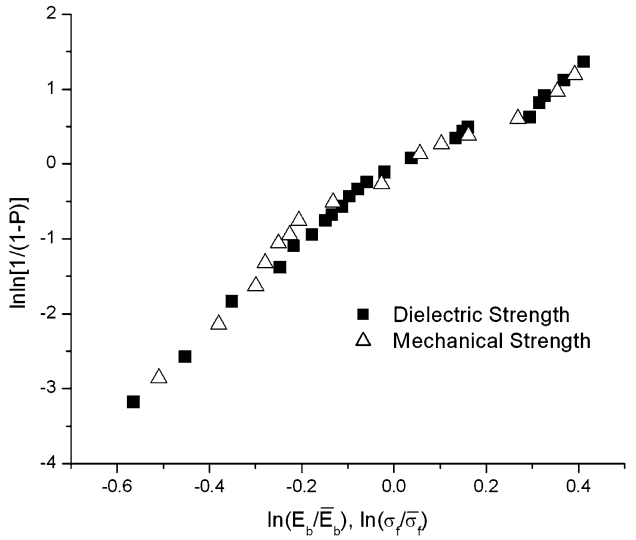

Fig. 4 Weibull plot of mechanical and electrical data for single dielectric layer $BaTiO_3$. (data from [14])

stand the differences in the results of the Weibull plots obtained in the present study, the failure origins in the capacitors must be determined.

Failure mechanisms

A strong correlation between mechanical failure and electrical breakdown was not found using Weibull statistics in the current study. SEM analysis was subsequently used to determine the origin of failure in the bars so that the causes of failure could be compared.

For bars that were tested mechanically, SEM results (Fig. 5a, b) show that failure due to flaws at the tensile surface of the mechanical test bars occurred in only 20% of the bars due to the polishing process prior to flexure testing. Velocity hackle and other fracture surface features were readily observed during SEM analysis. These lead back to the surface of the bar indicating that the surface was the origin of failure in these cases. Pores near the tensile surface of the flexure bars were also found as a second source of failure (Fig. 5c, d). These pores were readily observed during post-mortem SEM analysis. Failure in the polished bars was mainly caused by pores on, or near, the tensile surface, along with surface defects that were not removed by polishing.

The breakdown origins in the as-sintered bars that were used for electrical testing were also examined using SEM. Figure 6a and b shows a typical mode of failure: a pore between the electrode and dielectric layer that was observed in 40% of the bars that were tested to electrical breakdown. As predicted by modeling, a spherical pore in the material will result in a field enhancement in the material surrounding the pore approximately 1.5 times the applied field [22]. This field enhancement would be expected to lead to breakdown at the interface between the pore and the dielectric and to reduce the average breakdown strength of the material. A second type of breakdown mechanism that was observed in the bars produced in this study was breakdown at the electrode ends (Fig. 6c, d). This was the most prevalent breakdown mechanism observed in the study since 60% of the bars failed due to breakdown at the electrode ends. The electrode ends are also expected to exhibit a field enhancement effect; therefore, breakdown is more likely to occur at these points. In a parallel plate capacitor, the field is normal to the plates in the central region of the electrode, but extends into the dielectric beyond the electrode edges. This results in a field concentration at the edges. The resulting field at the electrode edges can be as much as twice the average field, thus leading to breakdown at this point [23]. Two different causes of failure have been observed in the bars produced in this study that were tested to mechanical and electrical failure. Failure due to pores was observed in both mechanical and electrical testing. In addition, failure at the electrode ends was also observed as a second mechanism for electrical failure.

Although pores were shown to cause both mechanical failure and electrical breakdown, the pores were located in different regions of the test bars. The pores close to the surface caused mechanical failure, whereas for electrical breakdown, failure often occurred at pores between the dielectric layers and the electrode layer in the volume of the sample, not in the surface region. The pores that caused mechanical failure in the samples were also found to be of varying size with some pores being relatively small (5 μm) and some pores as large as 30 μm. The pores that caused electrical failure could not be directly measured due to

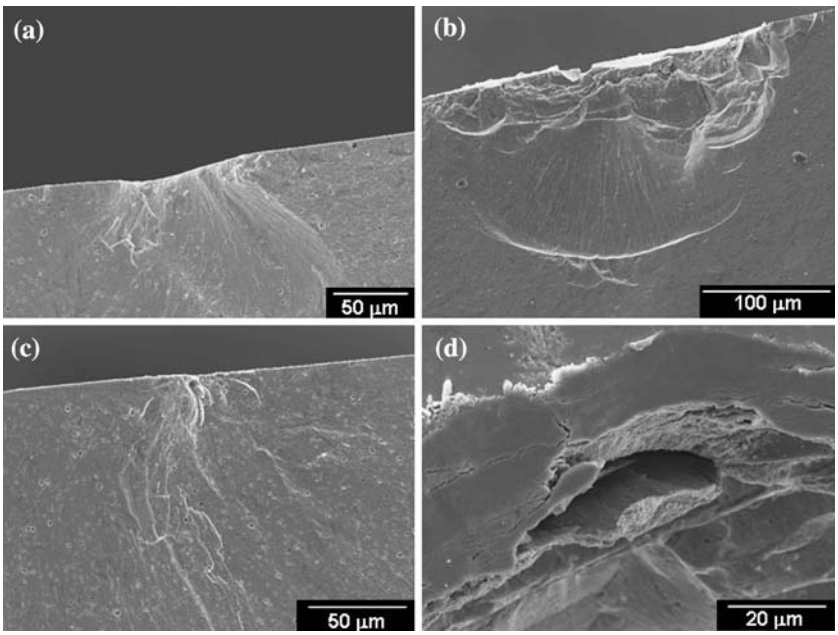

Fig. 5 SEM micrographs showing (**a**) and (**b**), failure initiating from flaws on the tensile surface of the bar and (**c**) and (**d**), failure initiating from a subsurface pore

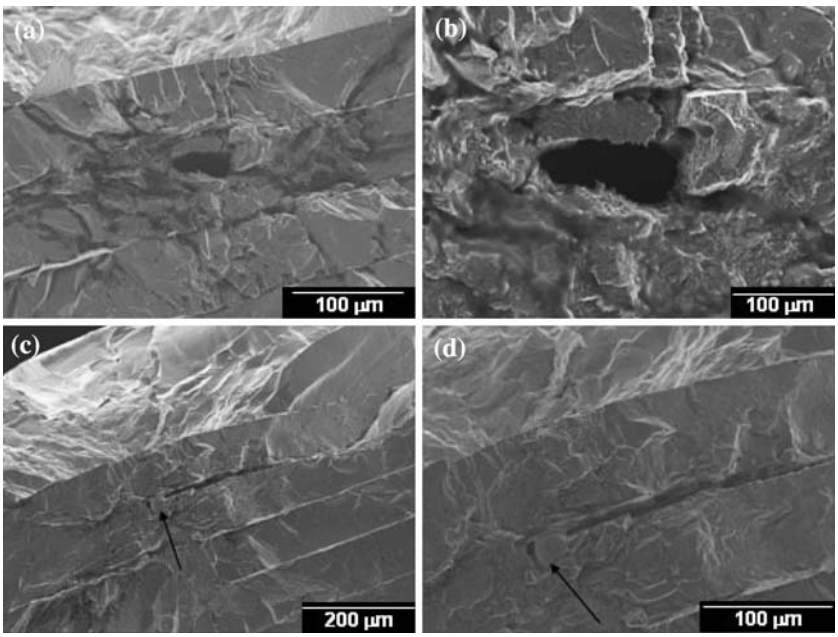

Fig. 6 SEM micrographs of electrical breakdown regions associated with a pore: (**a**) low magnification and (**b**) high magnification; and breakdown associated with an electrode end: (**c**) low magnification and (**d**) high magnification

some expansion of the pores as a result of catastrophic breakdown in that region of the capacitor. The different failure mechanisms found in the bars are an explanation for the differences in the Weibull distributions for both failure types. The failure mechanisms are not consistent between the two types of failure, and therefore, the Weibull plots would not be expected to show a strong correlation. The corresponding Weibull plots from the study by Kishimoto (Fig. 4 of ref. [18]) suggest that the origin of both mechanical and electrical failure would be expected to be the same. One difference between the results of Kishimoto and the current study is that the materials tested in the Kishimoto study were only one layer thick with terminations applied to the top and bottom of the layer. This would lead to a stronger correlation since pores between layers, electrode end effects and other factors that are present in a multilayer structure would not contribute to failure for such samples.

The slopes of the Weibull plots also support the observation that there is more than one type of failure origin causing mechanical and electrical failures. The Weibull plots that were obtained in this study and some of Ki-

shimoto's plots show multiple regions of varying slopes. A Weibull plot with discontinuities in the slope can be attributed to a mixture of failure modes [17]. The different slopes can be attributed to different failure mechanisms, such as pores and surface defects for mechanical failure and pores and electrode ends for electrical failure. The varying slope could also be attributed to flaws of different size controlling failure such as pores with two different size distributions or surface flaws of varying size. From the Weibull plots and the SEM images above, we can conclude that multiple failure mechanisms are causing failure in the capacitors, and therefore, there is not a direct correlation between mechanical and electrical failure in multilayer ceramic capacitors.

Conclusions

There is not a simple relationship between mechanical failure and electrical breakdown in high voltage, high energy density multilayer ceramic capacitors. Pores were the leading cause of both mechanical failure and electrical breakdown, but the location of the pores for mechanical versus electrical failure was different. Pores close to the surface of the capacitor resulted in mechanical failure, but did not contribute to electrical breakdown. Pores between the dielectric and electrode layers resulted in electrical breakdown, but did not play a major role in mechanical failure. Surface defects are a second kind of mechanical failure origin. The field enhancement associated with electrode ends provided a second mechanism for electrical breakdown. Overall, the mechanisms for mechanical and electrical failure were different when comparing failure events in working capacitors. Weibull statistics and microstructural analysis of failure origins were used to show that there is not a correlation between mechanical and electrical breakdown events in high voltage, high energy density multilayer capacitors examined in this study.

References

1. Lanagan M, Du J, Wang C, Moses P, Cheng C, Pan M (2001) IEEE 37:324
2. Sindeyev YG (1990) Ferroelectrics 110:193
3. Bunget I, Popescu M (1984) Physics of solid dielectrics, vol 19. Elsevier, Amsterdam
4. Hench LL, West JK (1990) Principles of electronic ceramics. John Wiley & Sons, New York, p 222
5. Anderson JC (1964) Dielectrics. Reinhold Publishing Corp., New York, p 98
6. Beauchamp EK (1959) J Amer Ceram Soc 54(10):1650
7. Gerson R (1959) J Appl Phys 30:1650
8. Bahn WA, Newnham RE (1986) Mater Res Bull 21:1073
9. Hench LL, West JK (1990) Principles of electronic ceramics. John Wiley & Sons, New York, p 222
10. Freiman WW, Pohanka RC (1989) J Amer Ceram Soc 72(12):2258
11. Moulson A, Herbert J (2003) Electroceramics, 2nd edn. John Wiley & Sons, New York, p 388
12. Dos Santos e Lucato SL, Lupascu DC, Kamlah M, Rodel J, Lynch CS (2001) Acta Mater 49:2751
13. Kasap SO (2002) Principles of electronic materials and devices, 2nd edn. The McGraw-Hill Companies, Inc., p 540
14. Wachtman JB (1996) Mechanical properties of ceramics. John Wiley & Sons, New York, p 15
15. Siemens Matsushita Components, Applications Bulletin 00050007 (2004)
16. Pohanka RC, Rice RW, Walker BE Jr (1976) J Amer Ceram Soc 59:1
17. Weibull W (1951) J Appl Mech 18:293
18. Kishimoto A (1989) J Mater Sci 24:698
19. Nakamura Y, Suzuki M, Motohira N, Kishimoto A, Yanagida H (1997) J Mater Sci 32:115
20. Al-Saffar R, Freer R, Tribick I, Ward P (1999) Br Ceram Proc 59:61
21. Kishi H, Mizuno Y, Chazono H (2003) Jpn J Appl Phys 42:1
22. Xu X (2004) Characterization of hexabarium 17-titanate and its effects on the dielectric properties of barium titanate ceramics. Ph.D. Dissertation, University of Missouri-Rolla, p 111
23. Moulson A, Herbert J (2003) Electroceramics, 2nd edn. John Wiley & Sons, New York, p 266